# Combined deficiencies of *Msx1* and *Msx2* cause impaired patterning and survival of the cranial neural crest

**Mamoru Ishii[1], Jun Han[2], Hai-Yun Yen[1], Henry M. Sucov[1], Yang Chai[2] and Robert E. Maxson, Jr[1,*]**

[1]Department of Biochemistry and Molecular Biology, Norris Cancer Hospital, Keck School of Medicine, University of Southern California, 1441 Eastlake Avenue, Los Angeles, CA 90089, USA
[2]Center for Craniofacial Molecular Biology, School of Dentistry, University of Southern California, 2250 Alcazar Street, CSA 103, Los Angeles, CA 90033, USA
*Author for correspondence (e-mail: maxson@hsc.usc.edu)

*Accepted 02 September 2005*

Development 132, 4937-4950
Published by The Company of Biologists 2005
doi:10.1242/dev.02072

## Summary

**The neural crest is a multipotent, migratory cell population that contributes to a variety of tissues and organs during vertebrate embryogenesis. Here, we focus on the function of *Msx1* and *Msx2*, homeobox genes implicated in several disorders affecting craniofacial development in humans. We show that *Msx1/2* mutants exhibit profound deficiencies in the development of structures derived from the cranial and cardiac neural crest. These include hypoplastic and mispatterned cranial ganglia, dysmorphogenesis of pharyngeal arch derivatives and abnormal organization of conotruncal structures in the developing heart. The expression of the neural crest markers *Ap-2α*, *Sox10* and cadherin 6 (*cdh6*) in *Msx1/2* mutants revealed an apparent retardation in the migration of subpopulations of preotic and postotic neural crest cells, and a disorganization of neural crest cells paralleling patterning defects in cranial nerves. In addition, normally distinct subpopulations of migrating crest underwent mixing. The expression of the hindbrain markers *Krox20* and *Epha4* was altered in *Msx1/2* mutants, suggesting that defects in neural crest populations may result, in part, from defects in rhombomere identity. *Msx1/2* mutants also exhibited increased *Bmp4* expression in migratory cranial neural crest and pharyngeal arches. Finally, proliferation of neural crest-derived mesenchyme was unchanged, but the number of apoptotic cells was increased substantially in neural crest-derived cells that contribute to the cranial ganglia and the first pharyngeal arch. This increase in apoptosis may contribute to the mispatterning of the cranial ganglia and the hypoplasia of the first arch.**

Key words: Neural Crest, Calvaria, Craniofacial, Cranial Ganglia, Cardiac outflow tract, *Msx1*, *Msx2*, Mouse embryo

## Introduction

The neural crest, a population of multipotent, migratory cells, plays a variety of crucial roles in vertebrate organogenesis (Gammill and Bronner-Fraser, 2003; Santagati and Rijli, 2003). Neural crest cells are first specified through an interaction between the neural plate and the adjacent non-neural ectoderm (Knecht and Bronner-Fraser, 2002; Meulemans and Bronner-Fraser, 2004). They later delaminate from the neural folds and migrate through the embryo laterally and ventrally, contributing to elements of the craniofacial apparatus, the peripheral nervous system, the cardiac outflow septum, and the endocrine glands. They are capable of differentiating into many tissue and cell types, including smooth muscle, bone, cartilage, tendon and melanocytes (Noden, 1983; Tan, 1986; Miyagawa-Tomita et al., 1991; Bronner-Fraser, 1993; Le Douarin and Kalcheim, 1999).

Combined human-genetic and molecular approaches have uncovered several genes required for neural crest development in humans and mice. These include transcription factors, cell adhesion molecules and molecules involved in cell-cell signaling (Wilkie and Morriss-Kay, 2001; Gammill and Bronner-Fraser, 2003; Halloran and Berndt, 2003; Santagati and Rijli, 2003). Most of the major signaling pathways, including Bmp, Wnt, Fgf, Shh, RA (retinoic acid) and ET (endothelin), have roles in neural crest development. Although these roles are increasingly well understood (Knecht and Bronner-Fraser, 2002; Gammill and Bronner-Fraser, 2003), it remains unclear how neural crest cells respond to and integrate signals from these pathways. One approach to this problem is to investigate the functions and interactions of the transcription factors that mediate the signals from these various pathways. Here, we focus on the Msx genes – effectors of Bmp, Wnt and Fgf signaling – and their roles in the development of subpopulations of neural crest that contribute to the craniofacial apparatus, cranial nerves, and cardiac outflow septum.

Msx genes form a subfamily within the Nk-like homeobox gene family (Gauchat et al., 2000; Pollard and Holland, 2000). Mammals possess three Msx genes, *Msx1*, *Msx2* and *Msx3* (Davidson, 1995; Shimeld et al., 1996; Wang et al., 1996). In vertebrates, *Msx1* and *Msx2* are known to act in a variety of cell types to control cell proliferation, differentiation (Woloshin et al., 1995; Liu et al., 1999;

Odelberg et al., 2000; Hu et al., 2001; Han et al., 2003; Ishii et al., 2003) and survival (Marazzi et al., 1997). From work in several vertebrate embryos and various organ systems, it has been shown that Msx genes function as downstream effectors of the Bmp pathway (Vainio et al., 1993; Marazzi et al., 1997; Bei and Maas, 1998; Hollnagel et al., 1999; Sirard et al., 2000; Daluiski et al., 2001; Bruggger et al., 2004). In addition, in some tissues, they serve as effectors of the Wnt and Fgf pathways (Chen et al., 1996; Montero et al., 2001; Willert et al., 2002; Hussein et al., 2003). *Msx1* and *Msx2* are expressed in premigratory and migratory neural crest, as well as in the neural crest-derived mesenchyme of the pharyngeal arches and median nasal process (Davidson, 1995; Bendall and Abate-Shen, 2000; Maxson et al., 2003). Recent studies in *Xenopus* and chicken showed that the forced expression of *Msx1* can induce neural crest marker expression in the dorsal aspect of embryos (Tribulo et al., 2003; Liu et al., 2004).

Mice homozygous for a targeted mutation in *Msx1* exhibit agenesis of the teeth, a cleft palate, and abnormalities of the cranial skeleton (Satokata and Maas, 1994). Tissue recombination experiments have shown that *Msx1* plays an essential role in epithelial-mesenchymal interactions during the tooth development (Chen et al., 1996; Bei and Maas, 1998). Han et al. provided evidence that *Msx1* also controls cell proliferation in the dental mesenchyme (Han et al., 2003). A defect in the development of the frontal bone is evident in mice homozygous for a targeted mutation in *Msx2*, mimicking key features of Familial Parietal Foramina (Satokata et al., 2000). We showed recently that the cause of this frontal bone defect includes deficiencies in the differentiation and proliferation of neural crest-derived calvarial osteogenic cells (Ishii et al., 2003). Mice with homozygous mutations in both *Msx1* and *Msx2* die in late gestation with severe craniofacial malformations, including exencephaly, cleft palate, agenesis of teeth, and unossified calvarial bones (Bei and Maas, 1998; Satokata et al., 2000). Although this spectrum of anomalies in *Msx1/2* mutants suggests a deficiency in the cranial neural crest, an analysis of neural crest development in such embryos has been lacking. Here, we report that *Msx1*$^{-/-}$*; Msx2*$^{-/-}$ embryos have defects not previously described in derivatives of the craniofacial and cardiac neural crest. These include hypoplasia and mis-patterning of the cranial ganglia, and anomalies in the conotruncus of the heart. The expression of neural crest markers in *Msx1/2* mutants revealed a delay in the migration of neural crest cells originating in r2, r4 and r6-r8. There was, in addition, a disorganization of the neural crest cells forming cranial ganglia, and a mixing of some subpopulations of neural crest, suggesting defects in neural crest compartment boundaries. Hindbrain marker gene expression suggested that Msx1/2 might affect rhombomere development. Finally, although the proliferation of neural crest-derived mesenchyme was unchanged in *Msx1/2* mutants, the number of apoptotic cells was elevated substantially in neural crest populations that contribute to the cranial ganglia and the first pharyngeal arch. These results suggest that *Msx1/2* act at several different steps of neural crest development, and in different neural crest subpopulations, to control the patterning of the craniofacial apparatus and cardiac outflow tract.

## Materials and methods

### Genotyping of *Msx1*$^{-/-}$*; Msx2*$^{-/-}$ mutant mice

*Msx1* and *Msx2* mutant mice have been described (Satokata and Maas, 1994; Satokata et al., 2000). Compound *Msx1*, *Msx2* heterozygotes (mixed genetic background of BALB/c and CD-1) were crossed to produce *Msx1*$^{-/-}$*; Msx2*$^{-/-}$ embryos. The noon copulation plug was counted as embryonic day 0.5. DNA was prepared either from yolk sac (embryos) or from tails (postnatal mice). *Msx1* and *Msx2* knockout alleles were identified by PCR. Primers and PCR conditions were as described (Satokata and Maas, 1994; Satokata et al., 2000).

### Immunostaining, analysis of skeletal morphology and detection of apoptotic cells

Whole-mount immunohistochemistry was carried out according to Mark et al. (Mark et al., 1993), using the 2H3 anti-neurofilament monoclonal antibody (1:500, Developmental Studies Hybridoma Bank). Primary antibody was followed by HRP-conjugated goat anti-mouse IgG antibody (1:100, Calbiochem). 4-chloro-1-naphtol chromogenic substrate (Sigma) was used for signal detection. Whole heads of E15.5 embryos were stained in PBS containing 1 μg/ml DAPI for 30 minutes and photographed under UV light. Detection of alkaline phosphatase and counterstaining with Nuclear Fast Red were as described (Liu et al., 1999). Whole-mount analysis of skeletal morphology was performed as described by McLeod (McLeod, 1980) and Hogan et al. (Hogan et al., 1994). For TUNEL identification of apoptotic cells, embryos were fixed in 4% paraformaldehyde and cryosectioned (10 μm). The In Situ Cell Death Detection Kit (Roche) was used according to the manufacturer's instructions. Sections were then treated with anti-phosphorylated Histone H3 polyclonal antibody (1/100, Upstate). then incubated with rhodamine-conjugated anti-rabbit IgG (1/100, Molecular Probes). Nuclei were counter-stained with DAPI. After Prolong (Molecular Probes) mounting, signals were photographed under fluorescence. Cell death was detected in whole embryos by Nile blue sulfate (Sigma), as described (Trumpp et al., 1999).

### In situ hybridization

Whole-mount in situ hybridization was performed according to Hogan et al. (Hogan et al., 1994). Conclusions were based on at least two independent experiments. Digoxigenin-labeled anti-sense RNA probes were visualized by BM-purple substrate (Roche). An *Msx1* 1.2 kb *Xho*I-*Xba*I cDNA fragment was subcloned into pSP72. An RNA probe was synthesized from the T7 promoter. Other RNA probes were generated as reported previously: *Ap-2α* (Mitchell et al., 1991), *Bmp4* (Wu et al., 2003), *cdh6* (Inoue et al., 1997), *Crabp1* (Stoner and Gudas, 1989), *Dlx5* (Depew et al., 1999), *Fgf8* (Crossley and Martin, 1995), *Epha4* (Nieto et al., 1992), *Hoxb1*, *Hoxd4* (Jiang et al., 2002), *Krox20* (Wilkinson et al., 1989), *Msx2*, *Twist* (Ishii et al., 2003), *Sox10* (Kuhlbrodt et al., 1998), *Tbx1* (Bollag et al., 1994) and *Wnt1* (Parr et al., 1993).

### *Wnt1-Cre*/*R26R* reporter assay

*Msx1* and *Msx2* mutants were crossed with *Wnt1-Cre* or *R26R* lines, producing embryos with the genotype *Msx1*$^{-/-}$*; Msx2*$^{-/-}$; *Wnt1-Cre*/+; *R26R*/+. β-Galactosidase analysis was carried out as described (Chai et al., 2000; Jiang et al., 2000).

## Results

### Gross morphological defects in *Msx1/2* mutant embryos

We crossed *Msx1*$^{+/-}$*; Msx2*$^{+/-}$ mutants and examined *Msx1*$^{-/-}$*; Msx2*$^{-/-}$ embryos at various stages of development (Fig. 1). A neural tube closure defect was apparent by E9.5, and some E9.5 embryos exhibited a flattened median nasal prominence. At E12.5, additional defects were visible, including thoraco-

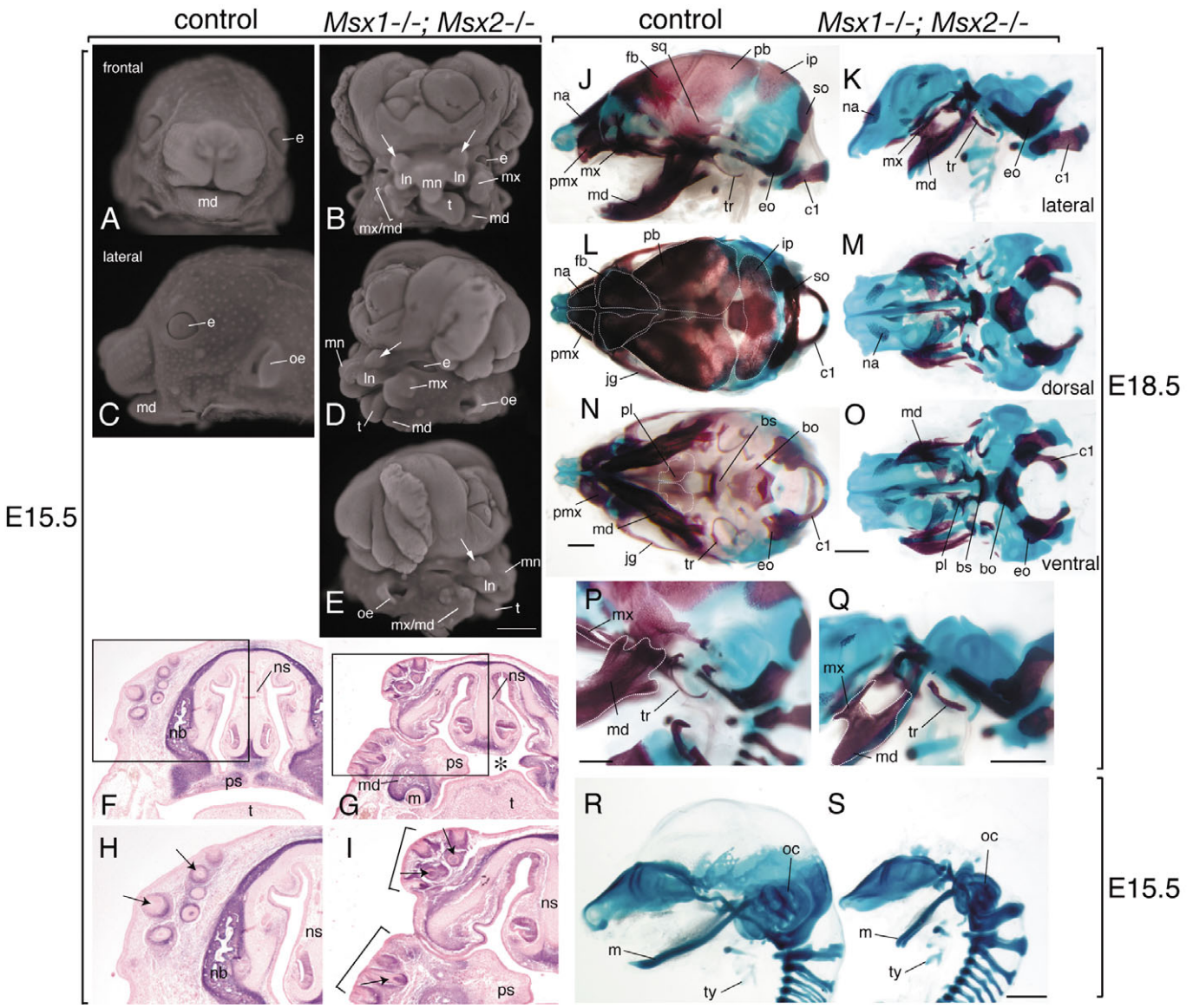


**Fig. 1.** Craniofacial dysmorphogenesis and skeletal abnormalities in *Msx1/2* compound mutant mice. (A-E) Craniofacial morphology of control (A,C) and *Msx1/2* double-mutant embryos (B,D,E) at E15.5. A and B show frontal views; C,D and E lateral views. *Msx1*$^{-/-}$*; Msx2*$^{-/-}$ embryos exhibit exencephaly, a hypoplastic maxilla, cleft mandible, and defects in the fusion of the median lateral, nasal and maxillary prominences. Arrows in B, D and E indicate the whisker pad. (F-I) Alkaline phosphatase stain of coronal sections of control (F,H) and mutant (G,I) embryos. Boxed areas in F and G are enlarged in H and I. *Msx1/2* mutants exhibit cleft palate (asterisk in G). Arrows in H and I indicate vibrissa follicles. Note, the mutant has divided whisker pads (brackets in I). (J-S) Skeletal analysis of *Msx1/2* compound mutants. (J-Q) E18.5 Alizarin Red/Alcian Blue-stained bone and cartilage. (J,L,N,P) Normal controls; (K,M,O,Q) *Msx1/2* mutants. (J,K,P,Q) Lateral views; (L,M) dorsal views; (N,O) ventral views. Note that a significant portion of the cranial skeletal components, including neural crest derivatives, is either missing or severely affected in mutant embryos. (P,Q) Fusion of hypoplastic mandible and maxilla is seen in the *Msx1/2* mutant (Q). Note that tympanic ring was also hypoplastic in the mutant. (R,S) Lateral views of Alcian Blue-stained control (R) and *Msx1/2* mutant (S) heads at E15.5. Note the parietal, supraoccipital and caudal processes of chondrocranium were absent in mutant. bo, basioccipital; bs, basisphenoid; c1, first cervical vertebra; e, eye; eo, exoccipital; fb, frontal bone; ip, interparietal bone; jg, jugal bone; ln, lateral nasal prominence; m, Meckel's cartilage; md, mandible; mn, median nasal prominence; mx, maxilla; na/nb, nasal bone; ns, nasal septum; oc, otic capsule; oe, outer ear; pb, parietal bone; pl, palatine; pmx, premaxilla; ps, palatal shelf; so, supraoccipital bone; sq, squamosal bone; t, tongue; tr, tympanic ring; ty, thyroid cartilage. Scale bars: 1 mm.

abdominoschisis (open body wall), malformed limb buds (data not shown), and a failure of the median nasal prominence to fuse with the lateral nasal and maxillary prominences. E15.5-E16.5 embryos had a hypoplastic maxilla, a cleft and shortened mandible (Fig. 1A-E), and spina bifida (with a penetrance of approximately 1 in 8; data not shown). At E15.5, embryos were pale and edematous, and had enlarged hearts. Few embryos survived to E18.5. Given that one out of 16 offspring of *Msx1*$^{+/-}$*; Msx2*$^{+/-}$ matings should have had the genotype *Msx1*$^{-/-}$*; Msx2*$^{-/-}$, we expected five such double homozygous mutants in the 87 embryos examined. Instead, we found only one, suggesting that most *Msx1/2* mutants die during embryogenesis (Table 1).

**Table 1. Frequency of *Msx1/2* compound mutants**

| Stage | Total* | *Msx1*$^{-/-}$ | *Msx2*$^{-/-}$ | *Msx1*$^{-/-}$;*Msx2*$^{+/-}$ | *Msx1*$^{+/-}$;*Msx2*$^{-/-}$ | *Msx1*$^{-/-}$;*Msx2*$^{-/-}$ (%) |
|---|---|---|---|---|---|---|
| E8.5 | 110 | 9 (8.2) | 7 (6.4) | 9 (8.2) | 11 (10.0) | 8 (7.3) |
| E9.5 | 815 | 48 (5.9) | 62 (7.6) | 103 (12.6) | 91 (11.2) | 47 (5.8) |
| E10.5 | 212 | 9 (4.2) | 6 (2.8) | 27 (12.7) | 24 (11.3) | 12 (5.7) |
| E12.5 | 237 | 10 (4.2) | 18 (7.6) | 26 (11.0) | 24 (10.1) | 13 (5.5) |
| E15.5 | 110 | 4 (3.6) | 10 (9.1) | 10 (9.1) | 19 (17.3) | 8 (7.3) |
| E16.5 | 81 | 6 (7.4) | 2 (2.5) | 18 (22.2) | 14 (17.3) | 5 (6.2) |
| E18.5 | 87 | 3 (3.4) | 9 (10.3) | 7 (8.0) | 9 (10.3) | 1 (1.1) |
| NB | 56 | 3 (5.4) | 8 (14.3) | 3 (5.4) | 11 (19.6) | 0 (0) |

*Total of all genotypes, including wild type, *Msx1*$^{+/-}$, *Msx2*$^{+/-}$, *Msx1*$^{+/-}$;*Msx2*$^{+/-}$, *Msx1*$^{-/-}$, *Msx2*$^{-/-}$, *Msx1*$^{-/-}$;*Msx2*$^{+/-}$, *Msx1*$^{+/-}$;*Msx2*$^{-/-}$, *Msx1*$^{-/-}$;*Msx2*$^{-/-}$.
NB, newborn.

## Defective development of structures derived from the cranial and cardiac neural crest in *Msx1*/2 mutant embryos

In *Msx1/2* mutants, the bones of the skull vault failed to develop (Satokata et al., 2000) (Fig. 1J-O). Because agenesis of the skull vault occurred even in embryos that did not have exencephaly, the skull vault defect was not a consequence of exencephaly. In E18.5 embryos, the tympanic ring was hypoplastic, and the maxilla and mandible were fused (Fig. 1P,Q). The parietal, supraoccipital and caudal processes of the chondrocranium were also deficient (Fig. 1R,S). Homeotic transformations were not evident in any skeletal elements (Fig. 1P-S, data not shown).

Afferent neurons and glial cells of the cranial and dorsal root ganglia are derived from the neural crest (Le Douarin and Kalcheim, 1999; Barlow, 2002). To examine the development of the cranial and dorsal root ganglia in *Msx1/2* null embryos, we performed whole-mount immunohistochemistry on E10.5 embryos using an anti-neurofilament antibody (Fig. 2). In all mutant embryos examined ($n$=4), the oculomotor nerve (III) was absent or disrupted, and the trigeminal ganglion (V) was significantly reduced in size (Fig. 2B-D). These data show that loss of *Msx1/2* resulted in hypoplasia and mispatterning of the cranial ganglia. The dorsal root ganglia, by contrast, were indistinguishable from wild type (data not shown). The proximal part of the IXth nerve was missing, and the distal portion of the IXth nerve was fused with the Xth nerve. An abnormal connection between the trigeminal and facial-acoustic nerves (VII-VIII) was evident in two embryos (Fig. 2B,C). The fusion of the IXth and Xth nerve was less dramatic in *Msx1*$^{-/-}$; *Msx2*$^{+/-}$ and in *Msx1*$^{+/-}$; *Msx2*$^{-/-}$ embryos than in *Msx1*$^{-/-}$; *Msx2*$^{-/-}$ embryos (Fig. 2E,F, data not shown), suggesting that patterning defects of the cranial nerve are Msx gene-dosage dependent.

Cardiac neural crest cells contribute to the cardiac outflow septum, and are required for the proper alignment of the aorta and pulmonary trunk (Kirby and Waldo, 1995). Although neither *Msx1* nor *Msx2* individual mutant mice exhibit defects in the development of the cardiac outflow tract (Kwang et al., 2002), all *Msx1/2* null mice that we examined ($n$=4) had conotruncal abnormalities, including double outlet right ventricle (DORV), Tetralogy of Fallot and persistent truncus arteriousus (PTA) (Fig. 3, data not shown). Each of these defects is attributable to defective neural crest development (Kirby and Waldo, 1995). In addition, double-mutant mice exhibited ventricular-septal defects (VSDs), hypoplastic valves, and dysmorphogenesis of the ventricular wall and myocardium (these defects will be described in detail elsewhere). Mutant hearts also contracted irregularly (data not shown), which, together with the finding of generalized edema, suggested that *Msx1*/2 null mutants had cardiac insufficiency. We did not detect conotruncal abnormalities in *Msx1*$^{-/-}$; *Msx2*$^{+/-}$ or *Msx1*$^{+/-}$; *Msx2*$^{-/-}$ embryos (data not shown).

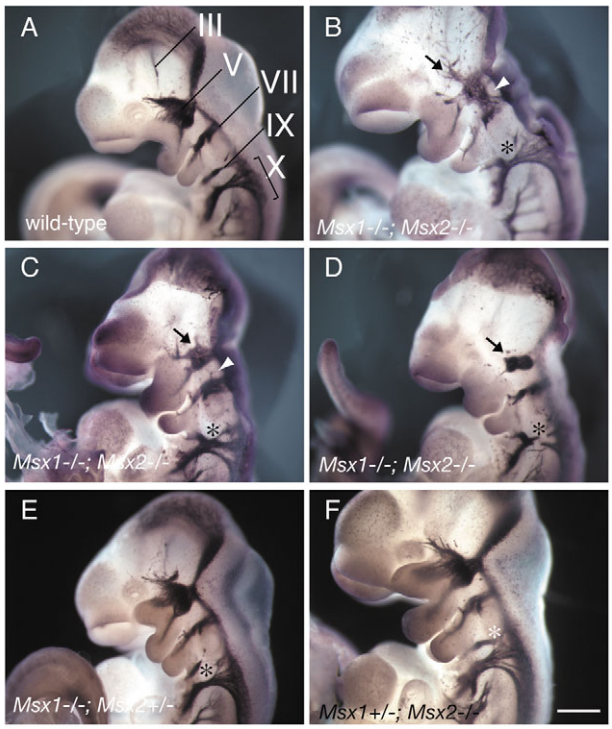


**Fig. 2.** Defects in neural crest-derived cranial ganglia in *Msx1/2* mutant embryos. (A-F) Whole-mount immunohistochemistry of neurofilament at E10.5. Control (A), *Msx1/2* double homozygous (B,C,D), *Msx1*$^{-/-}$; *Msx2*$^{+/-}$ (E), and *Msx1*$^{+/-}$; *Msx2*$^{-/-}$ (F) embryos. (B-D) Double homozygous mutant embryos show a hypoplastic trigeminal nerve (V; arrows), and fused glossopharyngeal (IX) and vagus (X) nerves in the distal portion (asterisk). An abnormal connection between the trigeminal and facial (VII) nerves can be observed in *Msx1/2* mutant embryos (arrowheads, B,C). Note the double-mutant embryo shown in D has impaired peripheral nerve growth and an interruption of the projection of the vagus nerve. The glossopharyngeal and vagus nerves were also fused in *Msx1*$^{-/-}$; *Msx2*$^{+/-}$ and *Msx1*$^{+/-}$; *Msx2*$^{-/-}$ embryos (asterisk, E,F). III, oculomotor nerve. Scale bar: 0.5 mm.

### Normal expression of marker genes in pharyngeal arches

The array of defects in *Msx1/2* mutant embryos suggested that the function of *Msx1* and *Msx2* is crucial for neural crest development. A simple hypothesis that would explain neural crest defects in *Msx1/2* mutants is that neural crest cells fail to populate target sites in the craniofacial region (Fig. 4). We used whole-mount hybridization to assess the expression of the neural crest markers *Ap-2α* (*Tcfap2a* – Mouse Genome Informatics), *Dlx5* and *Twist* in E9.0 and E9.5 embryos. *Ap-2α* is expressed in migratory cranial neural crest and in postmigratory crest in the pharyngeal arches (Mitchell et al., 1991). *Dlx5* and *Twist* are expressed in the first and second pharyngeal arches (Acampora et al., 1999; Depew et al., 1999; Wolf et al., 1991).

Each of these markers was expressed normally in the first and second arches (Fig. 4A-F), suggesting that the anomalies in neural crest-derived structures in the pharyngeal arches of *Msx1/2* mutants are not a result of large-scale deficiencies in the distribution of neural crest. Use of the *Wnt1-Cre/R26R* system (Chai et al., 2000; Jiang et al., 2000) to mark neural crest in *Msx1/2* mutants confirmed these findings (Fig. 4G,H).

### Delayed migration, mispatterning and inappropriate mixing of subpopulations of neural crest in *Msx1/2* mutant embryos

To determine whether more subtle changes in the specification or distribution of subpopulations of neural crest are responsible for the observed morphological defects, we examined the expression of marker genes at several stages of neural crest development (Figs 4-8). We used *Ap-2α* to assess neural crest development at E8.5. *Ap-2α* is normally expressed in crest cells in the neural folds and in migratory neural crest cells (Mitchell et al., 1991) (Fig. 4I,M).

At E8.5, the intensity of *Ap-2α* staining was reduced in the neural folds of pro-rhombomere B in the mutant (two out of two embryos; Fig. 4L,P). As demonstrated previously, *Msx1* and *Msx2* were both expressed in the neural folds and migratory neural crest in patterns that overlap with *Ap-2α* (Fig. 4Q-T). Although E8.5 *Msx1/2* mutant embryos had no detectable morphological abnormalities, these data suggest that loss of *Msx1/2* resulted in defects in the specification or distribution of subpopulations of cranial neural crest cells.

To assess neural crest development in embryos subsequent to E8.5, we continued to use *Ap-2α* (Figs 5, 6). We also used *cdh6* and *Sox10*, which are expressed in neural crest cells as they emigrate from the neural tube (Inoue et al., 1997; Southard-Smith et al., 1998).

At E9.5, *Msx1* and *Msx2* are expressed in the dorsal neural tube (Davidson, 1995) (Fig. 5A,B). Consistent with previous descriptions, *Ap-2α*, *cdh6* and *Sox10* were expressed in streams of neural crest migrating from r2 and r4 in the preotic hindbrain, and from r6-r8 in the postotic neural tube (Mitchell et al., 1991; Inoue et al., 1997; Southard-Smith et al., 1998) (Fig. 5C,E,G,I,K; Fig. 6A,C,E,G,I,K,M,O). *Ap-2α*, *cdh6* and *Sox10* expression was not detectable in r3 or r5, or in adjacent migratory crest cells (Fig. 5M,O, data not shown).

Differences in the expression of each of these three markers were evident in *Msx1/2* mutant embryos. *Ap-2α*, *cdh6* and *Sox10* were expressed ectopically in strips of cells located in normally neural crest-free areas adjacent to r3 (arrowhead in

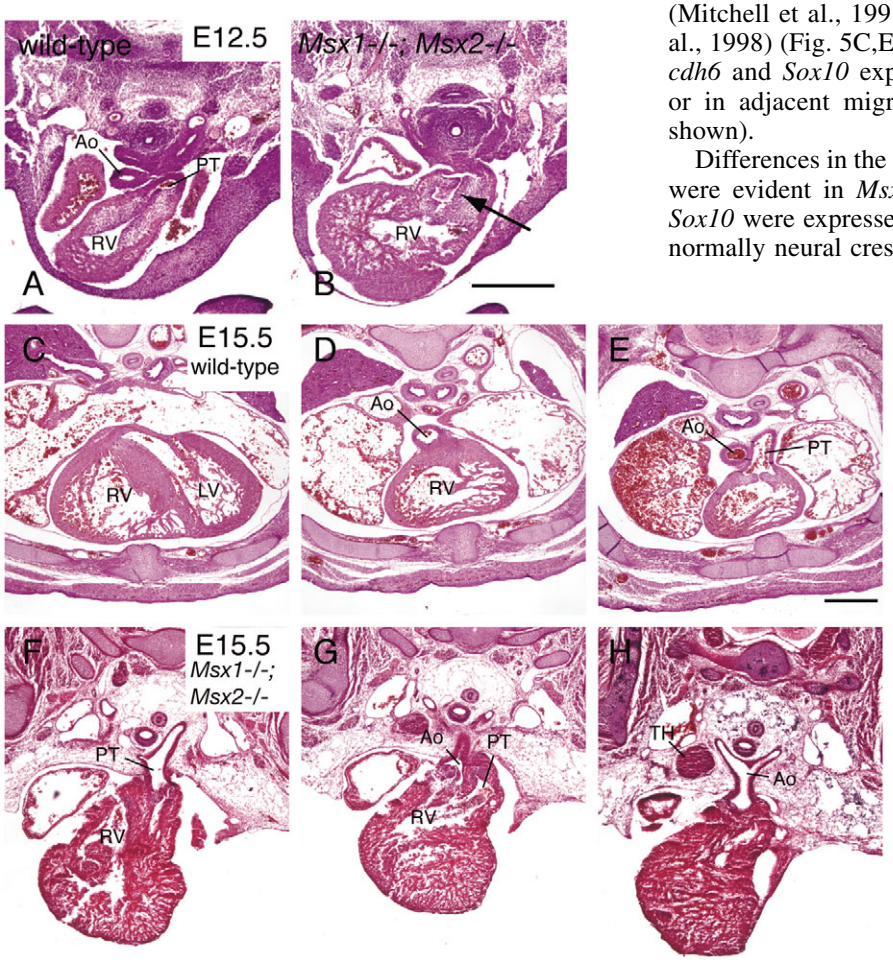


**Fig. 3.** Cardiac outflow tract defects in *Msx1/2* mutant embryos. Histological analysis of E12.5 (A,B) and E15.5 (C-H) control (A,C-E) and *Msx1/2* mutant (B,F-H) embryo hearts. (A,B) At E12.5, the septation of the pulmonary trunk (PT) and the ascending aorta (Ao) is evident in the control (A), but not in the mutant (arrow in B). (C-H) Serial transverse sections from caudal to rostral show the aorta and pulmonary trunk arising from the right ventricle in the mutant (double outlet right ventricle). *Msx1/2* mutants also exhibit dysmorphogenesis of the ventricular wall and myocardium. The location of the thymus (TH) was abnormal. RV, right ventricle; LV, left ventricle. Scale bars: in B, 0.5 mm for A,B; in E, 0.5 mm for C-H.

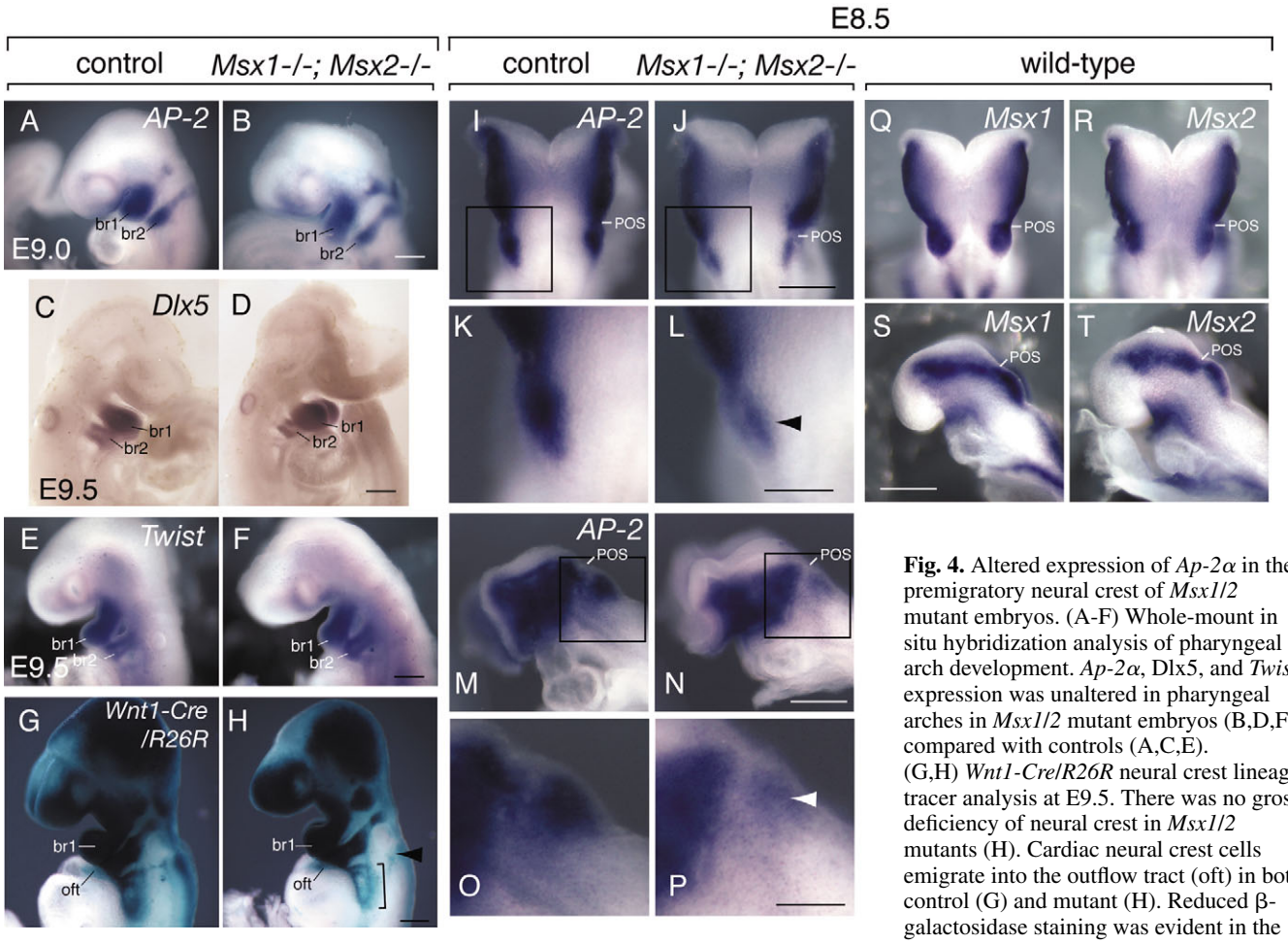


**Fig. 4.** Altered expression of *Ap-2α* in the premigratory neural crest of *Msx1/2* mutant embryos. (A-F) Whole-mount in situ hybridization analysis of pharyngeal arch development. *Ap-2α*, Dlx5, and *Twist* expression was unaltered in pharyngeal arches in *Msx1/2* mutant embryos (B,D,F) compared with controls (A,C,E). (G,H) *Wnt1-Cre/R26R* neural crest lineage tracer analysis at E9.5. There was no gross deficiency of neural crest in *Msx1/2* mutants (H). Cardiac neural crest cells emigrate into the outflow tract (oft) in both control (G) and mutant (H). Reduced β-galactosidase staining was evident in the peripharyngeal region (bracket) and in the stream of neural crest from r6 and r7 (arrowhead) in the mutant embryo. These differences may be due to the delayed timing of crest migration. (I-P) Analysis of premigratory and migratory neural crest development. Enlarged views of squares in I,J,M and N are shown in K,L,O and P. Expression of *Ap-2α* was significantly reduced in the neural fold caudal to the preotic sulcus in the mutant (arrowheads in L,P). (Q-T) In wild-type, the expression of *Msx1* and *Msx2* overlapped with that of *Ap-2α* at E8.5. pos, preotic sulcus; br1, first pharyngeal arch; br2, second pharyngeal arch. Scale bars: in B (for A,B), D (for C,D), F (for E,F), H (for G,H), J (for I,J), N (for M,N), S (for Q-T), 0.2 mm; in L (for K,L), P (for O,P), 0.1 mm.

Fig. 5D,H,J,L; Fig. 6B,F,H,N). Cross sections showed that for all three markers this expression was in mesenchyme (Fig. 5M-P, data not shown). These data suggest that, in *Msx1/2* mutants, neural crest cells were located abnormally in areas adjacent to r3.

In addition, *Ap-2α* was misexpressed in the dorsal neural tube and the adjacent mesenchyme at the levels of r2, r4 and r6-r8 (Fig. 5D,F,N,P; Fig. 6B,D,J). Because in normal embryos neural crest cells have already emigrated from the embryonic hindbrain by the 14-somite stage (Serbedzija, 1992), these data suggest that the combined loss of *Msx1/2* caused a significant retardation in the production, delamination or migration of a subpopulation of neural crest cells. Finally, *Ap-2α* and *Sox10* transcripts were reduced in the region of the trigeminal ganglion (Fig. 6B,F,J,N); there was also a reduction in the number of streams of postotic crest expressing these transcripts, from three to two (Fig. 6L,P). We detected *Ap-2α* expression in pharyngeal arches 3, 4 and 6 (Fig. 6D,L), suggesting that cardiac neural crest cells reach their target site in *Msx1/2* mutants.

### Altered expression of *Krox20* and *Epha4* but normal expression of *Hoxb1* and *Hoxd4* in hindbrains of *Msx1/2* mutant embryos

Changes in marker gene expression in cranial and cardiac neural crest populations raised the issue of whether loss of *Msx1* and *Msx2* affected rhombomere identity. We examined the expression of the hindbrain markers, *Krox20*, *Hoxb1*, *Hoxd4*, *Epha4* and *Crabp1* (Fig. 7). *Krox20* is expressed in r3 and r5 (Sham et al., 1993; Swiatek and Gridley, 1993). *Hoxb1* is expressed in r4 (Murphy et al., 1989), *Hoxd4* in the neural tube from r7 caudally (Morrison et al., 1997), and *Epha4* in r3 and r5 (Nieto et al., 1992). Gain- and loss-of-function experiments have shown that *Krox20*, *Hoxb1, Hoxd4* and *Epha4* are crucial for the establishment of rhombomere identity (Trainor and Krumlauf, 2000). *Crabp1* is expressed in r2 and throughout the hindbrain, from r4 to r6 (Maden et al., 1992).

Whole-mount stains with riboprobes for each of these markers revealed that *Krox20* was expressed normally in r3 in E8.5 mutants, but exhibited a restriction in the caudal limit of its expression in r5 (Fig. 7B,D). By E9.5, the r5 expression of

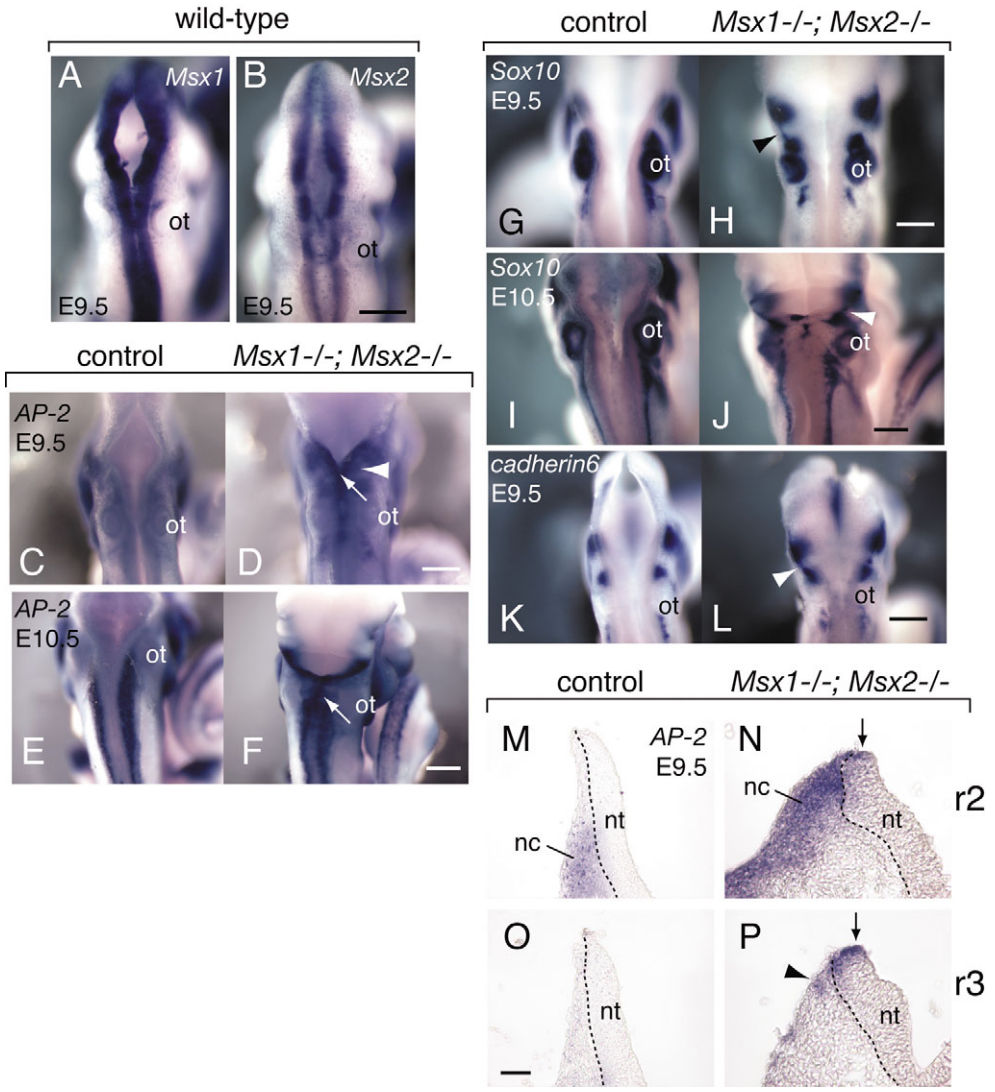


**Fig. 5.** Ectopic neural crest marker gene expression in the dorsal neural tube and mesenchyme cells adjacent to r3 of E9.5 *Msx1/2* mutant embryos. (A-L) Dorsal views of embryos analyzed by whole-mount in situ hybridization. (A,B) Expression of *Msx1* and *Msx2* in E9.5 wild-type embryos. (C-L) Expression of the neural crest markers *Ap-2α* (C-F), *Sox10* (G-J) and *cdh6* (K,L) in control (C,E,G,I,K) and *Msx1/2* mutant (D,F,H,J,L) embryos at the indicated stages. Note the aberrant expression of each marker at the level of r3 in mutant embryos (arrowheads in D,H,J,L). Intense ectopic expression of *Ap-2α* in the midline of the dorsal neural tube was also evident in mutant embryos (arrows in D,F). (M-P) Serial sections of *Ap-2α* stained whole-mount embryos. *Ap-2α* transcripts in the mutant are located in the mesenchyme adjacent to r3 (arrowhead in P). Arrows in N and P indicate ectopic *Ap-2α* expression in the dorsal neural tube of the mutant embryo. nc, neural crest; nt, neural tube; ot, otic vesicle. Scale bars: in B (for A,B), D (for C,D), H (for G,H), in L (for K,L), 0.2 mm: in F (for E,F), in J (for I,J), 0.4 mm; in O (for M-P), 50 μm.

*Krox20* was indistinguishable from that of wild type (Fig. 7F). The domains of expression of *Hoxb1*, *Hoxd4* and *Crabp1* were not altered in *Msx1/2* mutant embryos at E9.0 or E9.5 (Fig. 7H,J,L, data not shown). Intriguingly, however, *Epha4* expression was increased significantly in r3, and was expanded anteriorly into r1 and r2 (Fig. 7N,P). That hindbrain marker gene expression was unchanged in r4, r6 and r7 suggests that the defects in neural crest populations derived from these rhombomeres result from events downstream of the establishment of rhombomere identity. The changes in *Krox20* and *Epha4* expression suggest, however, that loss of *Msx1* and *Msx2* may at least transiently influence the development of r1, r2, r3 and r5.

### Msx genes are upstream of the extrinsic neural crest regulator *Bmp4*, but are not upstream of *Wnt1*, *Fgf8* or *Tbx1*

We next sought to identify deficiencies in signaling processes that might explain the abnormalities in subpopulations of neural crest. We examined the expression of three markers, *Wnt1*, *Fgf8* and *Tbx1* (Fig. 8). *Wnt1*, expressed in premigratory neural crest cells, is involved in neural crest expansion and subsequent differentiation (Ikeya et al., 1997; Saint-Jeannet et al., 1997). In the dorsal diencephalon of the mouse embryo, *Wnt1* expression depends on *Msx1* function (Bach et al., 2003). Expression of *Fgf8* in the isthmus, median nasal prominence and pharyngeal endoderm is required for the development of both cranial and cardiac neural crest (Abu-Issa et al., 2002; Frank et al., 2002; Trainor et al., 2002; Hu et al., 2003). Expression of *Fgf8* in pharyngeal arch ectoderm is important for the formation of the maxilla and mandible (Trumpp et al., 1999). *Tbx1*, required cell non-autonomously for neural crest cell migration in the third and fourth arch, functions upstream of *Fgf8*, and is a candidate for the cause of defective pharyngeal arch remodeling in DiGeorge/Velocardiofacial syndrome (Jerome and Papaioannou, 2001; Lindsay et al., 2001; Vitelli et al., 2002; Vitelli and Baldini, 2003). Bmps are expressed broadly in the pharyngeal ectoderm and endoderm, and are thought to influence the development of cranial and cardiac neural crest-lineage cells (Kanzler et al., 2000; Waldo et al., 2001; Ashique et al., 2002; Ohnemus et al., 2002). That *Bmp4* both regulates Msx genes and is itself regulated by them is well established (Chen et al., 1996; Bei and Maas, 1998; Zhang et al., 2003).

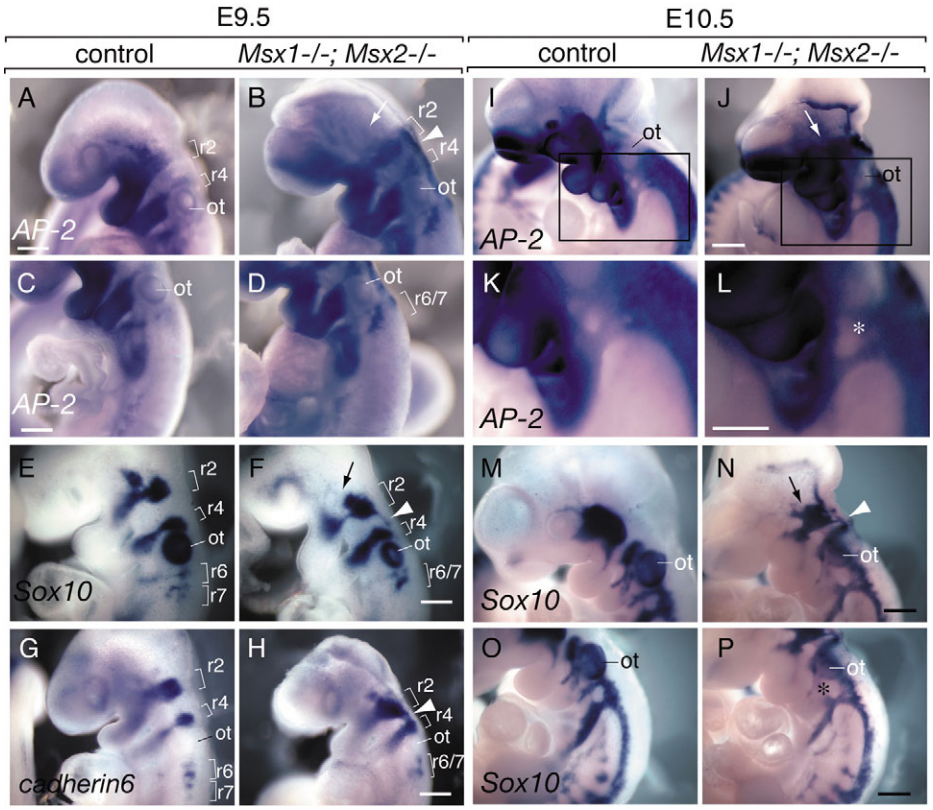


**Fig. 6.** Mispatterning and retarded migration of neural crest cells in E9.5-E10.5 *Msx1/2* mutant embryos. (A-P) Lateral views of E9.5 (A-H) and E10.5 (I-P) embryos hybridized with digoxigenin-labeled RNA probes for *Ap-2α* (A-D,I-L), *Sox10* (E,F,M-P) and *cdh6* (G,H). Note the abnormal expression in mutants of each marker at the level of r3, as indicated by arrowheads (B,F,H,N). Also note the retarded production and migration of neural crest cells from rhombomeres 2, 4, 6 and 7 at E9.5 (B,D). *Ap-2α* and *Sox10* expression in the trigeminal ganglion was significantly reduced (B,F,J,N arrows). In mutant embryos, merging of the migrating neural crest from r6 and r7 at E9.5 (D,F,H) results in the fusion of neural crest streams migrating into third and fourth arch arteries at E10.5 (asterisk in L,P). Boxed areas in I and J are shown at higher magnification in K and L. Scale bars: in A (for A,B), C (for C,D), F (for E,F), H (for G,H), 0.2 mm; in J (for I,J), L (for K,L), N (for M,N), P (for O,P), 0.4 mm.

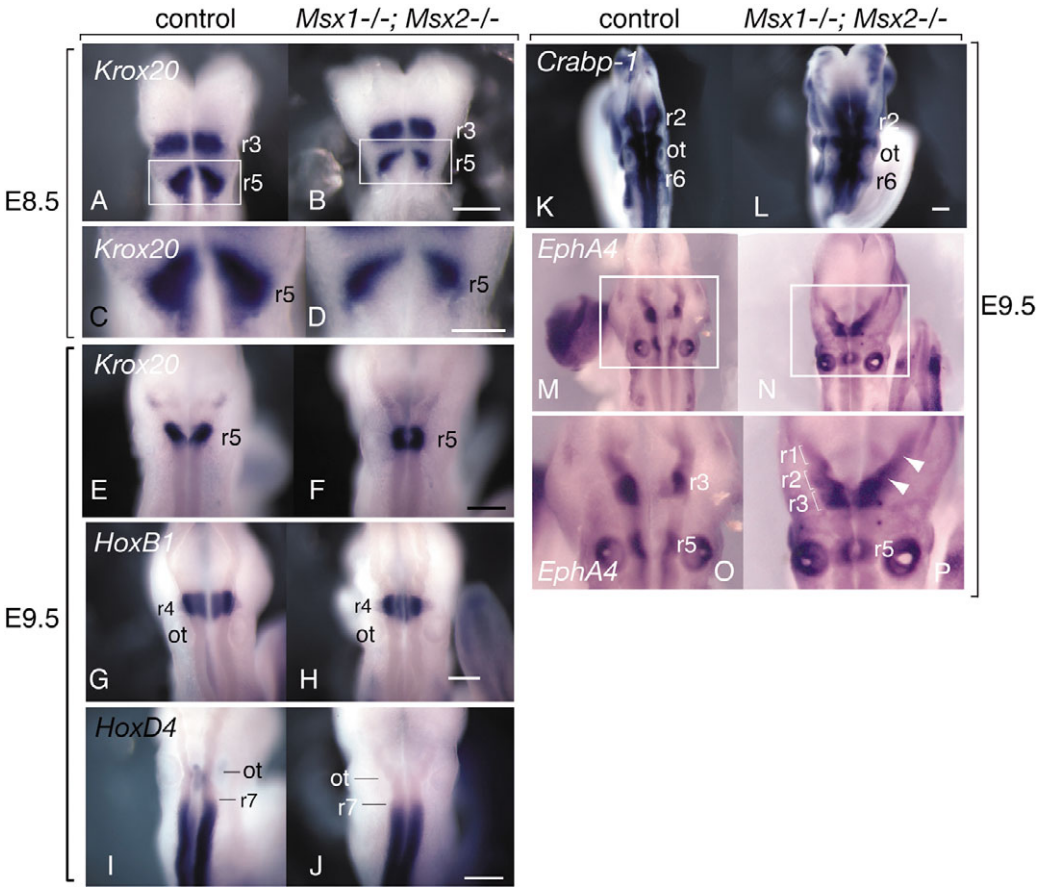


**Fig. 7.** Altered expression of *Krox20* and *Epha4* in *Msx1/2* mutant hindbrain. Whole-mount in situ hybridization analysis of E8.5 and E9.5 embryos with the indicated probes. (A-F) Expression of *Krox20* at E8.5 (A-D) and E9.5 (E,F). The box in A and B demarcates the region shown in C and D. Note the reduction in the level of *Krox20* transcripts in the caudal portion of r5 in mutant embryo at E8.5 (B,D), but normal expression at E9.5 (F). (G-L) Expression patterns of *Hoxb1* in r4 (G,H), *Hoxd4* in the region caudal to r7 (I,J), and *Crabp1* from r2 to r6 (K,L) at E9.5 show no apparent change in the mutant hindbrain. (M-P) *Epha4* expression at E9.5. Enlarged view of rectangles in M and N is shown in O and P. *Epha4* expression was significantly increased in r1, r2 and r3 of the *Msx1/2* mutant (arrowheads in P). Scale bars: in B (for A,B), F (for E,F), H (for G,H), J (for I,J), L (for K,L), 0.2 mm; D (for C,D), 0.1 mm.

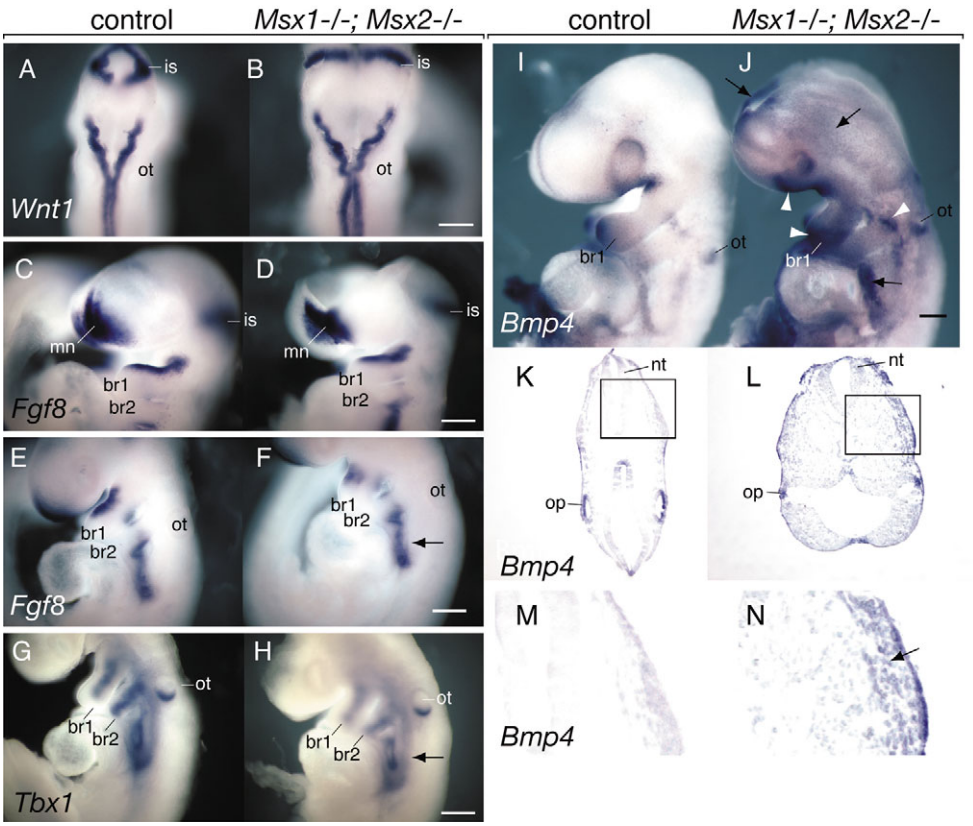


**Fig. 8.** Altered expression of Bmp4 in *Msx1/2* mutant embryos. (A,B) *Wnt1* expression was maintained in hindbrain, dorsal neural tube, and isthmus in *Msx1/2* double-mutant embryos. (C-F) Unchanged expression of *Fgf8* in the median nasal prominence (mn), isthmus (is) and pharyngeal arch1 in *Msx1/2* mutant (D,F) compared with control (C,E) embryos. Also note that expression of *Fgf8* (F) and *Tbx1* (H) in the peripharyngeal region was not significantly affected in the mutant (arrows). (I-N) *Bmp4* was upregulated in the forebrain, cranial mesenchyme, body wall epithelium (arrows), maxillary prominence, distal first pharyngeal arch, and proximal second pharyngeal arch (arrowhead). (K-N) Section analysis of *Bmp4* whole-mount embryos. Enlarged views of boxes in K and L are shown in M and N. The cranial mesenchyme and migratory neural crest (arrow in N) express *Bmp4* highly in *Msx1/2* mutants. Scale bars: in B (for A,B), D (for C,D), F (for E,F), H (for G,H), J (for I,J), 0.2 mm.

As is evident from results shown in Fig. 8B, the level of *Wnt1* expression in the isthmus and hindbrain of *Msx1/2* mutant embryos at E9.5 was comparable to that of control embryos. Similarly, *Fgf8* expression did not change in the isthmus, or in the median nasal prominence of *Msx1/2* mutant embryos at E9.5 (Fig. 8D,F). Nor did the distribution of *Tbx1* transcripts change significantly in pharyngeal endoderm or in the peripharyngeal region (Fig. 8H, data not shown). We note that expression of *Fgf8* in the first pharyngeal arch (Fig. 8F) and *Tbx1* in the mesodermal core of the pharyngeal arches (Fig. 8H) was slightly reduced in some mutant embryos.

E9.5 *Msx1/2* mutant embryos expressed *Bmp4* at significantly elevated levels in the cranial mesenchyme (including in migrating neural crest), the maxillary prominence, the distal part of the first pharyngeal arch, the proximal domain of the second pharyngeal arch, and the body wall epithelium (Fig. 8J,L,N, data not shown). These data suggest that Msx genes function downstream of, or in parallel to, *Wnt1*, *Fgf8* and *Tbx1*, but upstream of *Bmp4* during neural crest development.

### Increased apoptosis but unchanged proliferation in subpopulations of cranial neural crest in *Msx1*$^{-/-}$; *Msx2*$^{-/-}$ embryos

We next assessed apoptosis and proliferation in *Msx1/2* double-mutant embryos. Apoptosis was detected by a TUNEL assay, and proliferation by an antibody against 10-phosphorylated histone H3, which marks cells in M phase. These assays were carried out on the same cross sections of embryos. At E9.5, an increase in TUNEL-positive cells relative to controls was evident in the posterior prominence of the optic vesicle, as well as in the maxillary and mandibular prominences of the first pharyngeal arch (Fig. 9B,D,F). The majority of mesenchymal cells at these sites are derived from the cranial neural crest (Chai et al., 2000; Jiang et al., 2000). Whole-mount Nile Blue staining, which marks dying cells, confirmed these results (Fig. 9G-L). Concentrations of Nile Blue-positive cells were evident (1) in the area of the trigeminal ganglion (Fig. 9H, arrow), and (2) in the proximal (open arrowheads in Fig. 9H) and distal portions (arrowhead in Fig. 9H,J) of the first pharyngeal arch. No changes in TUNEL or Nile Blue staining were evident in the hindbrain or in migrating postotic neural crest cells (including cardiac neural crest) of *Msx1/2* mutants at E9.5 (Fig. 9J,L, data not shown).

We did not detect significant differences in the percentage of cells stained for phosphorylated histone H3 or BrdU in the pharyngeal arches or trigeminal ganglia (Fig. 9; data not shown). Consistent with the apparent lack of change in cell proliferation, counts of cell densities in the first pharyngeal arch showed no significant differences between *Msx1/2* mutants and control embryos (Fig. 9, data not shown). These results suggest that the combined loss of *Msx1* and *Msx2* influenced the survival but not the proliferation of subpopulations of neural crest-derived mesenchyme in the craniofacial region.

## Discussion

The neural crest is specified progressively, beginning at the time of its genesis in the neural tube, and continuing through its migration and later development in target tissues. Although this specification involves interactions between signaling

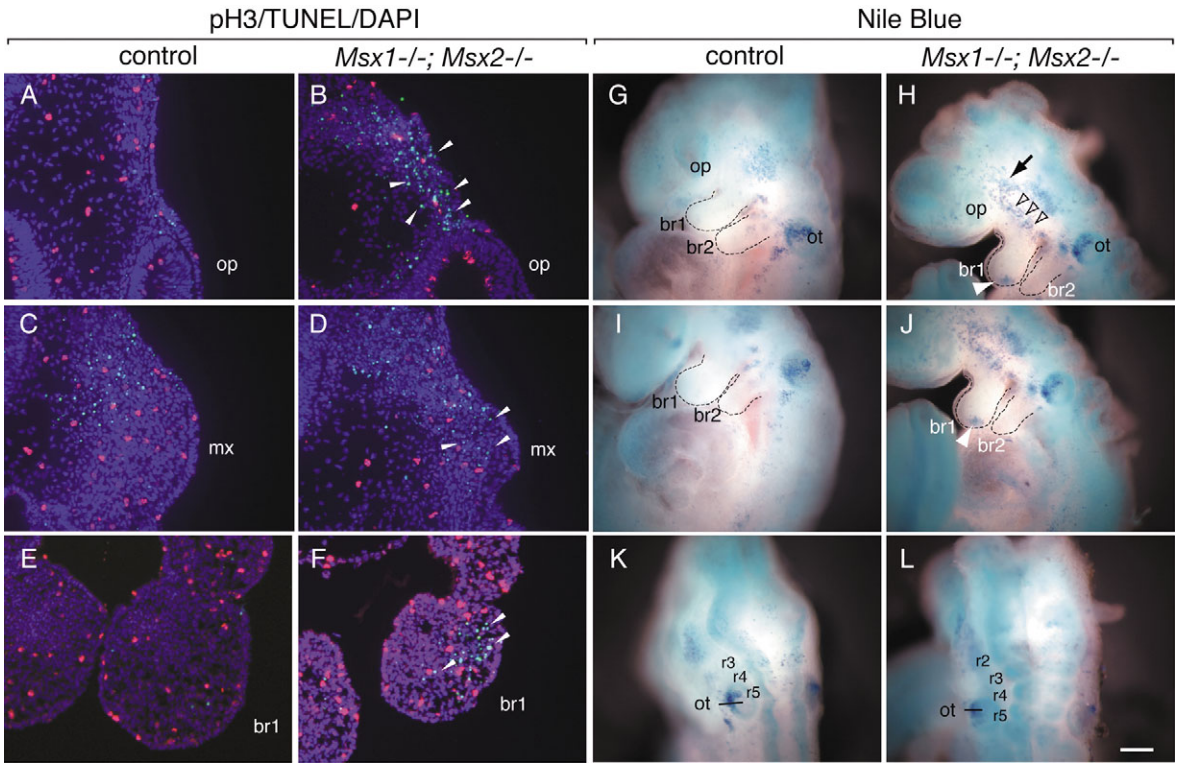


**Fig. 9.** *Msx1/2* are required for the survival of cranial neural crest cells. (A-F) Double-label immunostaining of apoptotic and proliferating cells. Immunostaining of phosphorylated histone H3 (Rhodamine, red) and TUNEL (FITC, green) were carried out on the same sections to detect cell proliferation and apoptosis in *Msx1/2* mutants. Nuclei were counterstained with DAPI. Arrowheads indicate increased apoptotic neural crest-derived cells in the region of the trigeminal ganglion (B), the proximal portion of pharyngeal arch1 (maxillary prominence; D), and the distal tip of pharyngeal arch1 (mandiblular prominence; F) of *Msx1/2* mutants at E9.5. Cell proliferation within these sites was not noticeably altered. (G-L) Nile Blue-stained E9.5 control (G,I,K) and *Msx1/2* mutant (H,J,L) embryos; lateral (G-J) and dorsal (K,L) views. Increased cell death was detected in neural crest-derived craniofacial structures of the *Msx1/2* mutant (arrows, arrowheads and open arrowheads in H and J) consistent with results of the TUNEL assay. We did not detect increased cell death in cardiac neural crest cells in mutant embryos (J). Note the lack of discernable change of cell death in the mutant hindbrain (L). Scale bar in L: 0.2 mm (for G-L).

pathways and downstream transcription factors, the molecular details of this process are not clear. The known functions of the Msx genes as effectors of the Bmp, Wnt and Fgf pathways, together with the well-documented role of these pathways in neural crest development, prompted us to undertake a close examination of neural crest development in *Msx1/2* mutants. We show that *Msx1/2* have major roles in several aspects of neural crest development, including the proper segregation of subpopulations of hindbrain neural crest, the patterning of the cranial ganglia and the survival of neural crest-derived cells in the pharyngeal arches.

### Msx gene function during the genesis and migration of neural crest cells

Several lines of evidence suggest that Msx genes are involved in the early events of neural crest specification. First, in the chick embryo, *Msx1* is expressed at the lateral edge of the neural plate, and *Msx1* expression at this site is dependent upon an interaction between neural and non-neural ectoderm (Streit and Stern, 1999). Second, the forced expression of *Msx1* in *Xenopus* embryos induces neural crest cells, and inhibition of *Msx1* activity by means of a dominant-negative form of *Msx1* inhibits the production of neural crest cells (Tribulo et al., 2003). Third, ectopic expression of *Msx1* in the neural tube of the chick can induce the expression of a neural crest cell marker (Liu et al., 2004). Despite the suggestion from these results that Msx genes have a crucial, early role in neural crest development, our data show that the majority of neural crest cells are induced, undergo migration, and populate the pharyngeal arches in the absence of *Msx1* and *Msx2*. We note, however, that the function of *Msx3*, which is expressed in the dorsal neural tube and in neural crest (Shimeld et al., 1996; Wang et al., 1996), may be sufficient for these activities. Thus, a definitive test of the role of Msx genes in murine neural crest development must await the simultaneous inactivation of *Msx1*, *Msx2* and *Msx3*.

Our results show that loss of *Msx1/2* results in the delayed appearance outside the neural tube of cells expressing neural crest markers. This is first evident in the expression of *Ap-2α* at E9.0, and is apparent at later stages in the expression of *cdh6* and *Sox10*. Whether this delay is due to a deficiency in the production, delamination or migration of neural crest cells remains unclear. A second intriguing anomaly is the partial merging or mixing of crest populations. Apparent in the expression patterns of *Ap-2α*, *cdh6* and *Sox10*, such mixing occurred between crest cells emigrating from r2 and those emigrating from r4, as well as between streams of crest emerging from the postotic rhombomeres 6, 7 and 8 (Figs 5,

6). DiI labeling will address the origin and migratory path of aberrant neural crest at the level of r3.

Krox20, kreisler (Mafb – Mouse Genome Informatics), and the combinatorial actions of Hox family members, establish and maintain boundaries between rhombomeres and between subpopulations of migrating neural crest cells. They do so, at least in part, by controlling the activities of Epha4 and Epha7 (Trainor and Krumlauf, 2000), which control cell-cell affinity. Reduced *Krox20* expression in r5 and increased *Epha4* from r1 to r3 of *Msx1/2* mutants suggests that *Msx1/2* may participate in rhombomere development. In normal embryos, neural crest is excluded from r3, whereas in *Msx1/2* mutants it is not. Upregulation of *Epha4* in Msx1/2 mutants may have some part in abrogating this exclusion. It is intriguing that in *Xenopus*, forced expression of a dominant-negative form of *Epha4* disrupted neural crest segregation (Smith et al., 1997). Overexpression of *Epha4* in *Msx1/2* mutants may have a dominant-negative effect and, as a consequence, may inhibit neural crest boundary formation between r2 and r4.

We consistently observed aberrant *Ap-2α* expression in the dorsal midline of *Msx1/2* mutant hindbrain from E9.0 through E10.5 (Fig. 5, data not shown). This may reflect a defect in the specification of a subpopulation of neural crest cells. *Msx1* and *Msx2*, as well as *Ap-2α* can maintain cells in an undifferentiated state (Liu et al., 1999; Odelberg et al., 2000; Hu et al., 2001; Pfisterer et al., 2002). That these three genes have similar functions, and that each is regulated by both Bmp and Wnt signals (Vainio et al., 1993; Willert et al., 2002; Luo et al., 2003), suggest that they may participate in a common molecular cascade in neural crest development. Also supporting this hypothesis is the striking similarity of phenotypes caused by the loss of *Msx1/2* and *Ap-2α*. Both mutants, for example, exhibit exencephaly, craniofacial skeletal defects, hypoplastic cranial ganglia, persistant truncus arteriosus and thoraco-abdominoschisis (open body wall) (Schorle et al., 1996; Zhang et al., 1996; Brewer et al., 2002). In *Ap-2α* mutants, as in *Msx1*/2 mutants, increases in the apoptosis of neural crest cells are likely to contribute to at least some defects in neural crest-derived structures (Schorle et al., 1996).

### *Msx1/2* are required for survival of neural crest subpopulations

Our results suggest that apoptosis may contribute to some of the morphological deficiencies of *Msx1/2* mutant embryos. The reduction in size of the trigeminal ganglion, as shown by decreased neurofilament expression, is preceded by a reduction of neural crest marker expression and a substantial increase in the number of apoptotic cells relative to control embryos (Fig. 9). Similarly, numbers of apoptotic cells are elevated in the maxillary prominence at E9.5. The mechanisms underlying this increase, including the issue of whether it is cell autonomous, remain unknown.

Previous work has shown that forced expression of *Msx2* can cause apoptosis in P19 cells and in the hindbrain of the chick embryo (Marazzi et al., 1997; Takahashi et al., 1998). A prediction of these overexpression experiments is that loss of *Msx1/2* should reduce apoptosis, which does not appear to be the case, either in the hindbrain or the pharyngeal arches. Although it is difficult to reconcile these results with ours, it is possible that the forced expression of Msx genes has a dominant-negative effect. Alternatively, the function of Msx genes may differ in cultured cells compared with in embryos, or in the chicken versus the mouse.

### Msx genes and pharyngeal arch development

We are intrigued by the finding that loss of *Msx1/2* function results in fusion of the maxillary and mandibular prominences, as well as in the reduced growth of these structures. Recent studies have shown that patterning of the craniofacial skeleton is controlled, in part, by non-Hox homeobox genes, including members of the Otx and Dlx families (Matsuo et al., 1995; Kuratani et al., 1997; Depew et al., 2002; Robledo et al., 2002). Because *Msx1* and *Msx2* are highly expressed in the maxillary prominence and mandibular arch, they could, in principle, function with other non-Hox homeobox genes in the axial patterning of craniofacial structures. In contradistinction to *Dlx5/Dlx6* knockout embryos, which exhibit a homeotic phenotype (Depew et al., 2002; Robledo et al., 2002), *Msx1/2* mutant embryos do not show evidence of homeotic transformations of craniofacial features. Although we have not systematically surveyed the expression of non-Hox homeobox genes in *Msx1/2* mutants, we have examined the expression of *Dlx5*, which is unaltered. This is consistent with the view that, in jaw development, the actions of *Msx1/2* either parallel that of *Dlx5* or are downstream of it. To the extent that a general function for Msx genes can be inferred from our data, such a function seems more likely to include the local control of cell segregation, differentiation and survival, than broad effects on region specification.

### Role of *Msx1*/2 in the developing heart

Neither the loss of *Msx1* nor *Msx2* individually causes outflow tract defects (Kwang et al., 2002). However, our results show that the combined loss of *Msx1* and *Msx2* results in major defects in the outflow tract in a high percentage of embryos. We did not detect significant changes in the expression of *Fgf8* or *Tbx1*, which function in the pharyngeal endoderm in signaling processes that influence cardiac crest development (Vitelli and Baldini, 2003). Similarly, the patterning of the caudal hindbrain from which the cardiac neural crest originates appeared to be largely normal in *Msx1/2* mutants, as assessed by the expression of *Hoxd4* and *Crabp1*. These results are consistent with our observation that cardiac neural crest cells are present in the pharyngeal arteries at E9.5 (Fig. 6). It will be interesting to determine whether these defects are caused by anomalies in the secondary heart field (Waldo et al., 2001), and whether they are crest-cell autonomous.

### Interaction between signaling pathways and Msx genes

Several upstream regulators of Msx genes have been identified. These include Bmps, Wnt/β-catenin and Fgf pathways. *Msx1/2* mutant embryos share features with mutants in each of these pathways (Ohnemus et al., 2002; Dâelot et al., 2003; Stottmann et al., 2004; Ikeya et al., 1997; Kioussi et al., 2002; Abu-Issa et al., 2002; Frank et al., 2002). The involvement of *Msx1/2* in multiple aspects of neural crest cell development implies that, depending on stage and tissue, Msx genes may function to integrate signals from several pathways.

Our results showed that *Bmp4* expression is increased in the cranial neural crest and pharyngeal arches of *Msx1/2* mutant

embryos. This suggests that Msx genes negatively control Bmp signals in these structures. Although, Msx genes do not appear to control the expression of *Wnt1* and *Fgf8* in neural crest development, it remains possible that there are additional signaling molecules regulated by Msx genes.

This work was supported by NIH Grants DE12941 and DE12450 to R.E.M., and DE014078 and DE012711 to Y.C. We thank Dr R. Maas for critical comments on the manuscript. For probes, we thank to Drs A. Baldini, T. Inoue, G. Martin, A. McMahon, J. Rubenstein, M. Wegner and T. Williams. The 2H3 antibody, developed by Drs J. Dodd and T. Jessell, was obtained from the Developmental Studies Hybridoma Bank maintained by the University of Iowa, Department of Biological Sciences, Iowa City, IA 52242, USA.

## References

**Abu-Issa, R., Smyth, G., Smoak, I., Yamamura, K. and Meyers, E. N.** (2002). *Fgf8* is required for pharyngeal arch and cardiovascular development in the mouse. *Development* **129**, 4613-4625.

**Acampora, D., Merlo, G. R., Paleari, L., Zerega, B., Postiglione, M. P., Mantero, S., Bober, E., Barbieri, O., Simeone, A. and Levi, G.** (1999). Craniofacial, vestibular and bone defects in mice lacking the Distal-less-related gene Dlx5. *Development* **126**, 3795-3809.

**Ashique, A. M., Fu, K. and Richman, J. M.** (2002). Endogenous bone morphogenetic proteins regulate outgrowth and epithelial survival during avian lip fusion. *Development* **129**, 4647-4660.

**Bach, A., Lallemand, Y., Nicola, M. A., Ramos, C., Mathis, L., Maufras, M. and Robert, B.** (2003). Msx1 is required for dorsal diencephalon patterning. *Development* **130**, 4025-4036.

**Barlow, L. A.** (2002). Cranial nerve development: placodal neurons ride the crest. *Curr. Biol.* **12**, R171-R173.

**Bei, M. and Maas, R.** (1998). FGFs and *BMP4* induce both *Msx1*-independent and *Msx1*-dependent signaling pathways in early tooth development. *Development* **125**, 4325-4333.

**Bendall, A. J. and Abate-Shen, C.** (2000). Roles for Msx and Dlx homeoproteins in vertebrate development. *Gene* **247**, 17-31.

**Bollag, R. J., Siegfried, Z., Cebra-Thomas, J. A., Garvey, N., Davison, E. M. and Silver, L. M.** (1994). An ancient family of embryonically expressed mouse genes sharing a conserved protein motif with the T locus. *Nat. Genet.* **7**, 383-389.

**Brewer, S., Jiang, X., Donaldson, S., Williams, T. and Sucov, H. M.** (2002). Requirement for *Ap-2*alpha in cardiac outflow tract morphogenesis. *Mech. Dev.* **110**, 139-149.

**Bronner-Fraser, M.** (1993). Mechanisms of neural crest cell migration. *BioEssays* **15**, 221-230.

**Brugger, S. M., Merrill, A. E., Torres-Vazquez, J., Wu, N., Ting, M. C., Cho, J. Y., Dobias, S. L., Yi, S. E., Lyons, K., Bell, J. R. et al.** (2004). A phylogenetically conserved cis-regulatory module in the Msx2 promoter is sufficient for BMP-dependent transcription in murine and Drosophila embryos. *Development* **131**, 5153-5165.

**Chai, Y., Jiang, X., Ito, Y., Bringas, P., Jr, Hn, J., Rowitch, D. H., Soriano, P., McMahon, A. P. and Sucov, H. M.** (2000). Fate of the mammalian cranial neural crest during tooth and mandibular morphogenesis. *Development* **127**, 1671-1679.

**Chen, Y., Bei, M., Woo, I., Satokata, I. and Maas, R.** (1996). *Msx1* controls inductive signaling in mammalian tooth morphogenesis. *Development* **122**, 3035-3044.

**Crossley, P. H. and Martin, G. R.** (1995). The mouse *Fgf8* gene encodes a family of polypeptides and is expressed in regions that direct outgrowth and patterning in the developing embryo. *Development* **121**, 439-451.

**Dâelot, E. C., Bahamonde, M. E., Zhao, M. and Lyons, K. M.** (2003). BMP signaling is required for septation of the outflow tract of the mammalian heart. *Development* **130**, 209-220.

**Daluiski, A., Engstrand, T., Bahamonde, M. E., Gamer, L. W., Agius, E., Stevenson, S. L., Cox, K., Rosen, V. and Lyons, K. M.** (2001). Bone morphogenetic protein-3 is a negative regulator of bone density. *Nat. Genet.* **27**, 84-88.

**Davidson, D.** (1995). The function and evolution of *Msx* genes: pointers and paradoxes. *Trends Genet.* **11**, 405-411.

**Depew, M. J., Liu, J. K., Long, J. E., Presley, R., Meneses, J. J., Pedersen, R. A. and Rubenstein, J. L.** (1999). Dlx5 regulates regional development of the branchial arches and sensory capsules. *Development* **126**, 3831-3846.

**Depew, M. J., Lufkin, T. and Rubenstein, J. L.** (2002). Specification of jaw subdivisions by Dlx genes. *Science* **298**, 381-385.

**Frank, D. U., Fotheringham, L. K., Brewer, J. A., Muglia, L. J., Tristani-Firouzi, M., Capecchi, M. R. and Moon, A. M.** (2002). An *Fgf8* mouse mutant phenocopies human 22q11 deletion syndrome. *Development* **129**, 4591-4603.

**Gammill, L. S. and Bronner-Fraser, M.** (2003). Neural crest specification: migrating into genomics. *Nat. Rev. Neurosci.* **4**, 795-805.

**Gauchat, D., Mazet, F., Berney, C., Schummer, M., Kreger, S., Pawlowski, J. and Galliot, B.** (2000). Evolution of Antp-class genes and differential expression of Hydra Hox/paraHox genes in anterior patterning. *Proc. Natl. Acad. Sci. USA* **97**, 4493-4498.

**Halloran, M. C. and Berndt, J. D.** (2003). Current progress in neural crest cell motility and migration and future prospects for the zebrafish model system. *Dev. Dyn.* **228**, 497-513.

**Han, J., Ito, Y., Yeo, J. Y., Sucov, H. M., Maas, R. and Chai, Y.** (2003). Cranial neural crest-derived mesenchymal proliferation is regulated by *Msx1*-mediated p19(INK4d) expression during odontogenesis. *Dev. Biol.* **261**, 183-196.

**Hogan, B., Beddington, R., Costantini, F. and Lacy, E.** (1994). *Manipulating the Mouse Embryo: A Laboratory Manual*. New York: Cold Spring Harbor Press.

**Hollnagel, A., Oehlmann, V., Heymer, J., Ruther, U. and Nordheim, A.** (1999). Id genes are direct targets of bone morphogenetic protein induction in embryonic stem cells. *J. Biol. Chem.* **274**, 19838-19845.

**Hu, D., Marcucio, R. S. and Helms, J. A.** (2003). A zone of frontonasal ectoderm regulates patterning and growth in the face. *Development* **130**, 1749-1758.

**Hu, G., Lee, H., Price, S. M., Shen, M. M. and Abate-Shen, C.** (2001). *Msx* homeobox genes inhibit differentiation through upregulation of cyclin D1. *Development* **128**, 2373-2384.

**Hussein, S. M., Duff, E. K. and Sirard, C.** (2003). Smad4 and beta-catenin co-activators functionally interact with lymphoid-enhancing factor to regulate graded expression of *Msx2*. *J. Biol. Chem.* **278**, 48805-48814.

**Ikeya, M., Lee, S. M., Johnson, J. E., McMahon, A. P. and Takada, S.** (1997). Wnt signalling required for expansion of neural crest and CNS progenitors. *Nature* **389**, 966-970.

**Inoue, T., Chisaka, O., Matsunami, H. and Takeichi, M.** (1997). *Cadherin-6* expression transiently delineates specific rhombomeres, other neural tube subdivisions, and neural crest subpopulations in mouse embryos. *Dev. Biol.* **183**, 183-194.

**Ishii, M., Merrill, A. E., Chan, Y. S., Gitelman, I., Rice, D. P., Sucov, H. M. and Maxson, R. E., Jr** (2003). *Msx2* and *Twist* cooperatively control the development of the neural crest-derived skeletogenic mesenchyme of the murine skull vault. *Development* **130**, 6131-6142.

**Jerome, L. A. and Papaioannou, V. E.** (2001). DiGeorge syndrome phenotype in mice mutant for the T-box gene, Tbx1. *Nat. Genet.* **27**, 286-291.

**Jiang, X., Rowitch, D. H., Soriano, P., McMahon, A. P. and Sucov, H. M.** (2000). Fate of the mammalian cardiac neural crest. *Development* **127**, 1607-1616.

**Jiang, X., Choudhary, B., Merki, E., Chien, K. R., Maxson, R. E. and Sucov, H. M.** (2002). Normal fate and altered function of the cardiac neural crest cell lineage in retinoic acid receptor mutant embryos. *Mech. Dev.* **117**, 115-122.

**Kanzler, B., Foreman, R. K., Labosky, P. A. and Mallo, M.** (2000). BMP signaling is essential for development of skeletogenic and neurogenic cranial neural crest. *Development* **127**, 1095-1104.

**Kioussi, C., Briata, P., Baek, S. H., Rose, D. W., Hamblet, N. S., Herman, T., Ohgi, K. A., Lin, C., Gleiberman, A., Wang, J. et al.** (2002). Identification of a Wnt/Dvl/beta-Catenin → Pitx2 pathway mediating cell-type-specific proliferation during development. *Cell* **111**, 673-685.

**Kirby, M. L. and Waldo, K. L.** (1995). Neural crest and cardiovascular patterning. *Circ. Res.* **77**, 211-215.

**Knecht, A. K. and Bronner-Fraser, M.** (2002). Induction of the neural crest: a multigene process. *Nat. Rev. Genet.* **3**, 453-461.

**Kuhlbrodt, K., Herbarth, B., Sock, E., Hermans-Borgmeyer, I. and Wegner, M.** (1998). Sox10, a novel transcriptional modulator in glial cells. *J. Neurosci.* **18**, 237-250.

**Kuratani, S., Matsuo, I. and Aizawa, S.** (1997). Developmental patterning

and evolution of the mammalian viscerocranium: genetic insights into comparative morphology. *Dev. Dyn.* **209**, 139-155.

**Kwang, S. J., Brugger, S. M., Lazik, A., Merrill, A. E., Wu, L. Y., Liu, Y. H., Ishii, M., Sangiorgi, F. O., Rauchman, M., Sucov, H. M. et al.** (2002). *Msx2* is an immediate downstream effector of Pax3 in the development of the murine cardiac neural crest. *Development* **129**, 527-538.

**Le Douarin, N. and Kalcheim, C.** (1999). *The Neural Crest.* Cambridge: Cambridge University Press.

**Lindsay, E. A., Vitelli, F., Su, H., Morishima, M., Huynh, T., Pramparo, T., Jurecic, V., Ogunrinu, G., Sutherland, H. F., Scambler, P. J. et al.** (2001). *Tbx1* haploinsufficieny in the DiGeorge syndrome region causes aortic arch defects in mice. *Nature* **410**, 97-101.

**Liu, Y. H., Tang, Z., Kundu, R. K., Wu, L., Luo, W., Zhu, D., Sangiorgi, F., Snead, M. L. and Maxson, R. E.** (1999). *Msx2* gene dosage influences the number of proliferative osteogenic cells in growth centers of the developing murine skull: a possible mechanism for *MSX2*-mediated craniosynostosis in humans. *Dev. Biol.* **205**, 260-274.

**Liu, Y., Helms, A. W. and Johnson, J. E.** (2004). Distinct activities of *Msx1* and *Msx3* in dorsal neural tube development. *Development* **131**, 1017-1028.

**Luo, T., Lee, Y. H., Saint-Jeannet, J. P. and Sargent, T. D.** (2003). Induction of neural crest in Xenopus by transcription factor AP2alpha. *Proc. Natl. Acad. Sci. USA* **100**, 532-537.

**Maden, M., Horton, C., Graham, A., Leonard, L., Pizzey, J., Siegenthaler, G., Lumsden, A. and Eriksson, U.** (1992). Domains of cellular retinoic acid-binding protein I (CRABP I) expression in the hindbrain and neural crest of the mouse embryo. *Mech. Dev.* **37**, 13-23.

**Marazzi, G., Wang, Y. and Sassoon, D.** (1997). *Msx2* is a transcriptional regulator in the *BMP4*-mediated programmed cell death pathway. *Dev. Biol.* **186**, 127-138.

**Mark, M., Lufkin, T., Vonesch, J. L., Ruberte, E., Olivo, J. C., Dolle, P., Gorry, P., Lumsden, A. and Chambon, P.** (1993). Two rhombomeres are altered in Hoxa-1 mutant mice. *Development* **119**, 319-338.

**Matsuo, I., Kuratani, S., Kimura, C., Takeda, N. and Aizawa, S.** (1995). Mouse Otx2 functions in the formation and patterning of rostral head. *Genes Dev.* **9**, 2646-2658.

**Maxson, R., Ishii, M. and Merrill, A.** (2003). Advances in Developmental Biology and Biochemistry. In *Murine Homeobox Gene Control of Embryonic Patterning and Organogeneis*, vol. 16 (ed. T. Lufkin), pp. 43-68. Amsterdam: Elsevier B.V.

**McLeod, M. J.** (1980). Differential staining of cartilage and bone in whole mouse fetuses by alcian blue and alizarin red S. *Teratology* **22**, 299-301.

**Meulemans, D. and Bronner-Fraser, M.** (2004). Gene-regulatory interactions in neural crest evolution and development. *Dev. Cell* **7**, 291-299.

**Mitchell, P. J., Timmons, P. M., Hâebert, J. M., Rigby, P. W. and Tjian, R.** (1991). Transcription factor AP-2 is expressed in neural crest cell lineages during mouse embryogenesis. *Genes Dev.* **5**, 105-119.

**Miyagawa-Tomita, S., Waldo, K., Tomita, H. and Kirby, M. L.** (1991). Temporospatial study of the migration and distribution of cardiac neural crest in quail-chick chimeras. *Am. J. Anat.* **192**, 79-88.

**Montero, J. A., Gaänan, Y., Macias, D., Rodriguez-Leon, J., Sanz-Ezquerro, J. J., Merino, R., Chimal-Monroy, J., Nieto, M. A. and Hurle, J. M.** (2001). Role of FGFs in the control of programmed cell death during limb development. *Development* **128**, 2075-2084.

**Morrison, A., Ariza-McNaughton, L., Gould, A., Featherstone, M. and Krumlauf, R.** (1997). *HOXD4* and regulation of the group 4 paralog genes. *Development* **124**, 3135-3146.

**Murphy, P., Davidson, D. R. and Hill, R. E.** (1989). Segment-specific expression of a homoeobox-containing gene in the mouse hindbrain. *Nature* **341**, 156-159.

**Nieto, M. A., Gilardi-Hebenstreit, P., Charnay, P. and Wilkinson, D. G.** (1992). A receptor protein tyrosine kinase implicated in the segmental patterning of the hindbrain and mesoderm. *Development* **116**, 1137-1150.

**Noden, D. M.** (1983). The role of the neural crest in patterning of avian cranial skeletal, connective, and muscle tissues. *Dev. Biol.* **96**, 144-165.

**Odelberg, S. J., Kollhoff, A. and Keating, M. T.** (2000). Dedifferentiation of mammalian myotubes induced by *Msx1*. *Cell* **103**, 1099-1109.

**Ohnemus, S., Kanzler, B., Jerome-Majewska, L. A., Papaioannou, V. E., Boehm, T. and Mallo, M.** (2002). Aortic arch and pharyngeal phenotype in the absence of BMP-dependent neural crest in the mouse. *Mech. Dev.* **119**, 127-135.

**Parr, B. A., Shea, M. J., Vassileva, G. and McMahon, A. P.** (1993). Mouse Wnt genes exhibit discrete domains of expression in the early embryonic CNS and limb buds. *Development* **119**, 247-261.

**Pfisterer, P., Ehlermann, J., Hegen, M. and Schorle, H.** (2002). A subtractive gene expression screen suggests a role of transcription factor AP-2 alpha in control of proliferation and differentiation. *J. Biol. Chem.* **277**, 6637-6644.

**Pollard, S. L. and Holland, P. W.** (2000). Evidence for 14 homeobox gene clusters in human genome ancestry. *Curr. Biol.* **10**, 1059-1062.

**Robledo, R. F., Rajan, L., Li, X. and Lufkin, T.** (2002). The Dlx5 and Dlx6 homeobox genes are essential for craniofacial, axial, and appendicular skeletal development. *Genes Dev.* **16**, 1089-1101.

**Saint-Jeannet, J. P., He, X., Varmus, H. E. and Dawid, I. B.** (1997). Regulation of dorsal fate in the neuraxis by *Wnt-1* and Wnt-3a. *Proc. Natl. Acad. Sci. USA* **94**, 13713-13718.

**Santagati, F. and Rijli, F. M.** (2003). Cranial neural crest and the building of the vertebrate head. *Nature reviews. Neuroscience* **4**, 806-818.

**Satokata, I. and Maas, R.** (1994). *Msx1* deficient mice exhibit cleft palate and abnormalities of craniofacial and tooth development. *Nat. Genet.* **6**, 348-356.

**Satokata, I., Ma, L., Ohshima, H., Bei, M., Woo, I., Nishizawa, K., Maeda, T., Takano, Y., Uchiyama, M., Heaney, S. et al.** (2000). *Msx2* deficiency in mice causes pleiotropic defects in bone growth and ectodermal organ formation. *Nat. Genet.* **24**, 391-395.

**Schorle, H., Meier, P., Buchert, M., Jaenisch, R. and Mitchell, P. J.** (1996). Transcription factor AP-2 essential for cranial closure and craniofacial development. *Nature* **381**, 235-238.

**Serbedzija, G. N., Bronner-Fraser, M. and Fraser, S. E.** (1992). Vital dye analysis of cranial neural crest cell migration in the mouse embryo. *Development* **116**, 297-307.

**Sham, M. H., Vesque, C., Nonchev, S., Marshall, H., Frain, M., Gupta, R. D., Whiting, J., Wilkinson, D., Charnay, P. and Krumlauf, R.** (1993). The zinc finger gene *Krox20* regulates HoxB2 (Hox2.8) during hindbrain segmentation. *Cell* **72**, 183-196.

**Shimeld, S. M., McKay, I. J. and Sharpe, P. T.** (1996). The murine homeobox gene *Msx*-3 shows highly restricted expression in the developing neural tube. *Mech. Dev.* **55**, 201-210.

**Sirard, C., Kim, S., Mirtsos, C., Tadich, P., Hoodless, P. A., Itie, A., Maxson, R., Wrana, J. L. and Mak, T. W.** (2000). Targeted disruption in murine cells reveals variable requirement for Smad4 in transforming growth factor beta-related signaling. *J. Biol. Chem.* **275**, 2063-2070.

**Smith, A., Robinson, V., Patel, K. and Wilkinson, D. G.** (1997). The EphA4 and EphB1 receptor tyrosine kinases and ephrin-B2 ligand regulate targeted migration of branchial neural crest cells. *Curr. Biol.* **7**, 561-570.

**Southard-Smith, E. M., Kos, L. and Pavan, W. J.** (1998). *Sox10* mutation disrupts neural crest development in Dom Hirschsprung mouse model. *Nat. Genet.* **18**, 60-64.

**Stoner, C. M. and Gudas, L. J.** (1989). Mouse cellular retinoic acid binding protein: cloning, complementary DNA sequence, and messenger RNA expression during the retinoic acid-induced differentiation of F9 wild type and RA-3-10 mutant teratocarcinoma cells. *Cancer Res.* **49**, 1497-1504.

**Stottmann, R. W., Choi, M., Mishina, Y., Meyers, E. N. and Klingensmith, J.** (2004). BMP receptor IA is required in mammalian neural crest cells for development of the cardiac outflow tract and ventricular myocardium. *Development* **131**, 2205-2218.

**Streit, A. and Stern, C. D.** (1999). Establishment and maintenance of the border of the neural plate in the chick: involvement of FGF and BMP activity. *Mech. Dev.* **82**, 51-66.

**Swiatek, P. J. and Gridley, T.** (1993). Perinatal lethality and defects in hindbrain development in mice homozygous for a targeted mutation of the zinc finger gene *Krox20*. *Nat. Rev. Neurosci.* **7**, 2071-2084.

**Takahashi, K., Nuckolls, G. H., Tanaka, O., Semba, I., Takahashi, I., Dashner, R., Shum, L. and Slavkin, H. C.** (1998). Adenovirus-mediated ectopic expression of *Msx2* in even-numbered rhombomeres induces apoptotic elimination of cranial neural crest cells in ovo. *Development* **125**, 1627-1635.

**Tan, S. S. and Morriss-Kay, G. M.** (1986). Analysis of cranial neural crest cell migration and early fates in postimplantation rat chimaeras. *J. Embryol. Exp. Morph.* **98**, 21-58.

**Trainor, P. A. and Krumlauf, R.** (2000). Patterning the cranial neural crest: hindbrain segmentation and Hox gene plasticity. *Nat. Rev. Neurosci.* **1**, 116-124.

**Trainor, P. A., Ariza-McNaughton, L. and Krumlauf, R.** (2002). Role of the isthmus and FGFs in resolving the paradox of neural crest plasticity and prepatterning. *Science* **295**, 1288-1291.

**Tribulo, C., Aybar, M. J., Nguyen, V. H., Mullins, M. C. and Mayor, R.** (2003). Regulation of *Msx* genes by a Bmp gradient is essential for neural crest specification. *Development* **130**, 6441-6452.

**Trumpp, A., Depew, M. J., Rubenstein, J. L., Bishop, J. M. and Martin, G. R.** (1999). Cre-mediated gene inactivation demonstrates that *FGF8* is required for cell survival and patterning of the first branchial arch. *Genes Dev.* **13**, 3136-3148.

**Vainio, S., Karavanova, I., Jowett, A. and Thesleff, I.** (1993). Identification of BMP-4 as a signal mediating secondary induction between epithelial and mesenchymal tissues during early tooth development. *Cell* **75**, 45-58.

**Vitelli, F. and Baldini, A.** (2003). Generating and modifying DiGeorge syndrome-like phenotypes in model organisms: is there a common genetic pathway? *Trends Genet.* **19**, 588-593.

**Vitelli, F., Taddei, I., Morishima, M., Meyers, E. N., Lindsay, E. A. and Baldini, A.** (2002). A genetic link between *Tbx1* and fibroblast growth factor signaling. *Development* **129**, 4605-4611.

**Waldo, K. L., Kumiski, D. H., Wallis, K. T., Stadt, H. A., Hutson, M. R., Platt, D. H. and Kirby, M. L.** (2001). Conotruncal myocardium arises from a secondary heart field. *Development* **128**, 3179-3188.

**Wang, W., Chen, X., Xu, H. and Lufkin, T.** (1996). *Msx3*: a novel murine homologue of the Drosophila *msh* homeobox gene restricted to the dorsal embryonic central nervous system. *Mech. Dev.* **58**, 203-215.

**Wilkie, A. O. and Morriss-Kay, G. M.** (2001). Genetics of craniofacial development and malformation. *Nat. Rev. Genet.* **2**, 458-468.

**Wilkinson, D. G., Bhatt, S., Chavrier, P., Bravo, R. and Charnay, P.** (1989). Segment-specific expression of a zinc-finger gene in the developing nervous system of the mouse. *Nature* **337**, 461-464.

**Willert, J., Epping, M., Polack, J. R., Brown, P. O. and Nusse, R. A.** (2002). A transcriptional response to Wnt protein in human embryonic carcinoma cells. *BMC Dev. Biol.* **2**, 8.

**Wolf, C., Thisse, C., Stoetzel, C., Thisse, B., Gerlinger, P. and Perrin-Schmitt, F.** (1991). The M-*Twist* gene of Mus is expressed in subsets of mesodermal cells and is closely related to the Xenopus X-twi and the Drosophila *Twist* genes. *Dev. Biol.* **143**, 363-373.

**Woloshin, P., Song, K., Degnin, C., Killary, A. M., Goldhamer, D. J., Sassoon, D. and Thayer, M. J.** (1995). *MSX1* inhibits myoD expression in fibroblast x 10T1/2 cell hybrids. *Cell* **82**, 611-620.

**Wu, L. Y., Li, M., Hinton, D. R., Guo, L., Jiang, S., Wang, J. T., Zeng, A., Xie, J. B., Snead, M., Shuler, C. et al.** (2003). Microphthalmia resulting from MSX2-induced apoptosis in the optic vesicle. *Investigative Ophthalmol. Vis. Sci.* **44**, 2404-2412.

**Zhang, J., Hagopian-Donaldson, S., Serbedzija, G., Elsemore, J., Plehn-Dujowich, D., McMahon, A. P., Flavell, R. A. and Williams, T.** (1996). Neural tube, skeletal and body wall defects in mice lacking transcription factor AP-2. *Nature* **381**, 238-241.

**Zhang, Z., Song, Y., Zhang, X., Tang, J., Chen, J. and Chen, Y.** (2003). *Msx1*/*Bmp4* genetic pathway regulates mammalian alveolar bone formation via induction of Dlx5 and Cbfa1. *Mech. Dev.* **120**, 1469-1479.